Geometrical Optics of Magnetoelastic Wave Propagation in a Nonuniform Magnetic Field

By B. A. AULD

(Manuscript received July 21, 1964)

The propagation of magnetoelastic waves in a magnetic insulator having a nonuniform internal magnetic field is examined in the geometrical optics approximation. Hamilton's ray path equations are obtained from the slowness relation for the medium, and it is shown that for YIG there is a substantial focusing action in the rod configuration commonly used for magnetic delay line experiments. When external field shaping is used to produce a minimum internal field at the midpoint of the rod it is found that divergence of the magnetoelastic waves is to be expected.

I. INTRODUCTION

In a number of experiments,[1,2,3] propagation of magnetoelastic waves has been observed in discs and rods of yttrium iron garnet. Coupling is provided through an internal field variation along the direction of propagation, radially in a disc and axially in a rod. This permits excitation of the wave in a region of small wave vector,[4,5] where the magnetic field can couple to the magnetization, with subsequent tapering into the magnetoelastic crossover region. The demagnetizing field also varies in magnitude and in orientation across the direction of propagation. In regions where the wave vector is large it is appropriate to consider the effects of this field inhomogeneity in terms of geometrical optics, and it is to be expected that refraction of the magnetoelastic waves will occur.

II. THE SLOWNESS RELATION AND GROUP VELOCITY

In a cubic crystal with a dc magnetic field applied along a [100] axis x_3 and, for simplicity, assumed elastically isotropic propagation of magnetoelastic waves is governed by the set of equations[6]

$$
\begin{aligned}
i\omega M_{x_1} + \omega_{H_k} M_{x_2} - i\gamma bk \cos\theta\, R_{t'} &= 0 \\
(\omega_{H_k} + \omega_M \sin^2\theta) M_{x_1} - i\omega M_{x_2} - i\gamma bk(\cos 2\theta\, R_t + \sin 2\theta\, R_l) &= 0 \\
(\omega^2 - c_t^2 k^2) R_t - i(bk/\rho M) \cos 2\theta\, M_{x_1} &= 0 \qquad (1) \\
(\omega^2 - c_t^2 k^2) R_{t'} - i(bk/\rho M) \cos\theta\, M_{x_2} &= 0 \\
(\omega^2 - c_l^2 k^2) R_l - i(bk/\rho M) \sin 2\theta\, M_{x_1} &= 0,
\end{aligned}
$$

where

$$
\begin{aligned}
\omega_{H_k} &= \gamma(H + H_{ex} a^2 k^2) \\
\omega_M &= \gamma 4\pi M.
\end{aligned}
$$

The wave vector $\bar{\mathbf{k}}$ is assumed to lie in a (100) plane at an angle θ with the dc field. M_{x_1}, M_{x_2} are transverse components of the magnetic moment referred to axes along [100] directions, and $R_{t'}$, R_t, R_l are transverse and longitudinal components of elastic displacement. The saturation magnetization is denoted by M and the mass density by ρ. Transverse and longitudinal elastic wave velocities are represented by c_t and c_l respectively, and b is the second magnetoelastic constant, generally designated by b_2. H is the internal dc magnetic field, H_{ex} is the exchange field, and a the lattice constant. In what follows it will be assumed that the crystal has sufficient magnetoelastic isotropy ($b_1 \approx b_2$) that (1) is valid for a magnetic field applied at a small angle to the [100] axis and for propagation in any azimuthal direction.

Upon elimination of variables in (1), the secular equation is found to be

$$
\begin{aligned}
\Omega(\omega,k,\theta) = (\omega_s^2 - \omega^2) - \frac{(bk)^2}{\rho M H_k} \\
\cdot\left\{\frac{\omega^2 \cos^2\theta}{\omega_{td}^2 - \omega^2} + \frac{\omega_{H_k} \cos^2 2\theta}{\omega_t^2 - \omega^2} + \frac{\omega_{H_k}^2 \sin^2 2\theta}{\omega_l^2 - \omega^2}\right\} = 0
\end{aligned} \qquad (2)
$$

where

$$
\begin{aligned}
\omega_s^2 &= \omega_{H_k}(\omega_{H_k} + \omega_M \sin^2\theta) \\
\omega_{td}^2 &= \omega_t^2 - \frac{(bk)^2}{\rho M H_k} \cos^2\theta \\
\omega_t^2 &= c_t^2 k^2 \\
\omega_l^2 &= c_l^2 k^2.
\end{aligned}
$$

This equation relates the wave vector $\mathbf{k}$ or the wave slowness vector $\mathbf{k}/\omega = \mathbf{k}/kv_{ph}$ to ω and θ, a relation which may be displayed graphically by a dispersion diagram (see Fig. 1). In coordinates k_1, k_2, k_3 the slowness relation (2) defines a "wave vector" [7] or "slowness" [8] surface for each value of ω. Since the magnetoelastic dispersion curves (see Fig. 1) have four branches and the dispersion relation is independent of azimuthal angle, the wave vector surface is a surface of revolution about x_3 and comprises four sheets. For example, a vertical section through the sheet of the wave vector surface corresponding to branch III appears, at $\omega \approx \omega_H$, as shown in Fig. 2. The group velocity vector[7]

$$\mathbf{V}_g = \nabla_k \omega = -\frac{\nabla_k \Omega}{\partial \Omega / \partial \omega} \tag{3}$$

is proportional to the gradient of Ω and is therefore normal to the wave vector surface, as shown in Fig. 2, the sense of the normal being determined by the requirement that the angle between $\mathbf{V}_g$ and $\mathbf{k}$ be less than $\pi/2$. This means that except in the special cases $\theta = 0$ or $\pi/2$, the group velocity vector is not exactly parallel to the wave vector; and a wave packet does not move in a direction normal to its phase fronts, a phenomenon which is characteristic of anisotropic media.

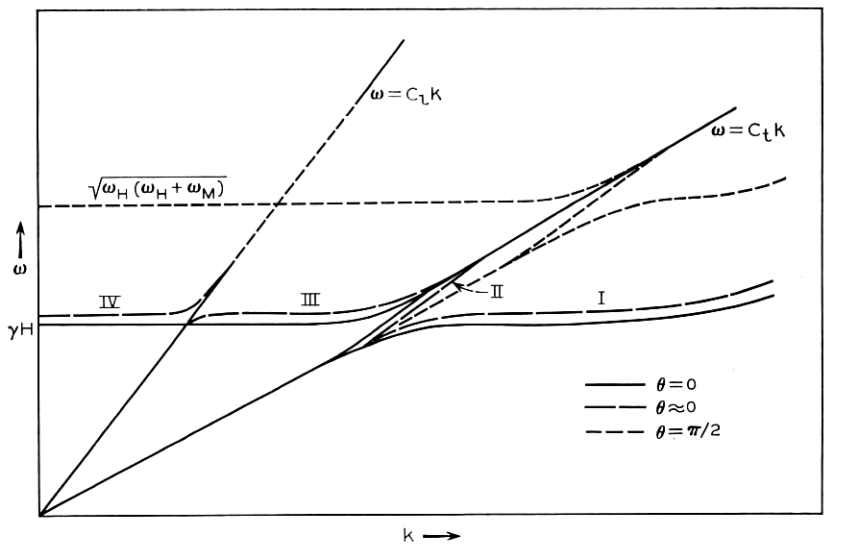

Fig. 1 — Magnetoelastic dispersion diagram.

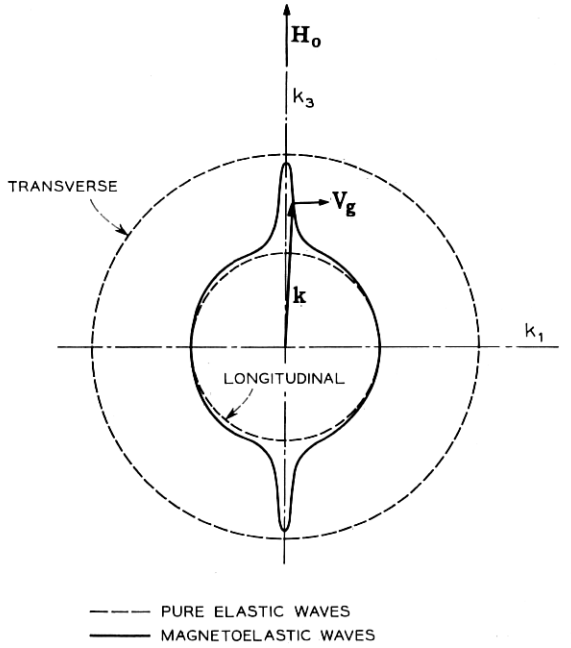

Fig. 2 — Wave vector surface for branch III of the dispersion diagram, at $\omega \approx \omega_H$.

III. THE EIKONAL EQUATION AND THE RAY EQUATIONS

It is assumed that the magnetic field varies in both magnitude and direction from point to point in the medium, but is sufficiently strong at all points to saturate the magnetization. The geometrical optics approximation is appropriate when the magnetic field is almost constant over regions comparable with a wavelength in dimension, so that a solution to the magnetoelastic equations having the form

$$\mathbf{M}(\mathbf{r})e^{i\psi(\mathbf{r})}$$

$$\mathbf{R}(\mathbf{r})e^{i\psi(\mathbf{r})}$$

appears over a small region as a plane wave with relatively slowly varying amplitude. If the assumed solutions are introduced into the equations of motion and spatial derivatives of **R** and **M** are neglected, equations (1) are obtained with $|\nabla\psi|$ substituted for $|k|$, and the angle between the "local" wave vector $\nabla\psi$ and the local magnetic field is substituted for θ. With the same substitutions, the slowness relation (2) reduces to a first-order partial differential equation for the phase function ψ,

$$\Omega(\omega, p_i, x_i) = 0$$

$$p_i = \frac{\partial \psi}{\partial x_i}, \qquad i = 1, 2, 3. \tag{4}$$

This is the eikonal equation or equation of geometrical optics. In the neighborhood of a singularity of the medium the approximations made in deriving the eikonal equation sometimes break down.[9] For the case of electromagnetic propagation in a ferrite, Seidel[10] has shown that singularities of this kind occur because of the appearance of logarithmic derivate coefficients in the field equation. It is not clear whether similar singularities exist for the magnetoelastic equations, and no attempt will be made to justify rigorously the use here of the geometrical optics approximation.

The standard method of solving (4) is by means of the characteristic or ray equations[11]

$$dx_i/dw = \partial\Omega/\partial p_i \tag{5a}$$

$$dp_i/dw = -\partial\Omega/\partial x_i, \tag{5b}$$

where w is a parameter. For any set of initial values of p_i, x_i satisfying (4) these equations, which form the basis of Hamiltonian optics,[8,12] define a unique curve in the space x_1, x_2, x_3. The significance of this curve becomes clear when the equivalence of p_i to the component k_i of the "local" wave vector is recalled. This shows [from (3)] that the tangent,

$$(dx_1 : dx_2 : dx_3) = \left(\frac{\partial\Omega}{\partial p_i} : \frac{\partial\Omega}{\partial p_2} : \frac{\partial\Omega}{\partial p_3}\right),$$

to any curve defined by (4) and a set of initial conditions is always collinear with the group velocity vector. Therefore the curve, or *ray path*, obtained by integrating (5) describes the trajectory of a wave packet launched at a specified point x_i with a specified "local" wave vector $k_i = p_i$. The value of the phase function ψ at any point on the ray path is obtained implicitly from

$$\frac{d\psi}{dw} = p_1 \frac{\partial\Omega}{\partial p_1} + p_2 \frac{\partial\Omega}{\partial p_2} + p_3 \frac{\partial\Omega}{\partial p_3}, \tag{6}$$

where [from (5a)] dw is related to the increment in ray path length ds through the relation

$$ds = \left\{\left(\frac{\partial\Omega}{\partial p_1}\right)^2 + \left(\frac{\partial\Omega}{\partial p_2}\right)^2 + \left(\frac{\partial\Omega}{\partial p_3}\right)^2\right\}^{\frac{1}{2}} dw.$$

When the wave vector surface has more than one sheet there are several initial group velocities corresponding to the same initial wave vector *direction*. These are distinguished by the magnitude of the initial wave vector, and a wave packet will therefore trace out different ray paths according to the magnitude of the initial wave vector, each path corresponding in a local sense to propagation in a mode associated with a particular branch of the dispersion diagram. When there is only a slow spatial variation of the magnetic field there will be little coupling between modes and the different ray paths will maintain their distinct identities.

The present discussion will be concerned with ray paths corresponding to branches I and III of the dispersion diagram. In this case Schlömann[6] has shown that, in the region where the uncoupled magnetic and transverse elastic waves cross, the slowness relation can be written approximately as

$$(\omega - \omega_s)(\omega - c_t k) - (\sigma/2)\omega_{cr} f(\theta) = 0,$$

where $\sigma = \gamma b^2/\alpha M$, ω_{cr} is the crossover frequency for the uncoupled waves, α is the elastic stiffness c_{44}, and

$$f(\theta) = \tfrac{1}{2}[(2 - 5\sin^2\theta + 4\sin^4\theta)(1 + \tfrac{1}{4}\omega_M{}^2\omega_s{}^{-2}\sin^4\theta)^{\frac{1}{2}} + \tfrac{1}{2}\omega_M\omega_s{}^{-1}\sin^4\theta(3 - 4\sin^2\theta)].$$

At the lower microwave frequencies it can be shown that the k dependence of ω_s due to exchange has a very much smaller effect on the slope of the dispersion curves than does the magnetoelastic coupling. If exchange is neglected

$$\omega_{cr} = \omega_s = \omega_H\left(1 + \frac{\omega_M}{\omega_H}\sin^2\theta\right)^{\frac{1}{2}},$$

in which $\omega_H = \gamma H$ and the eikonal equation takes the form

$$\Omega(\omega, p_i, x_i) = (p_1{}^2 + p_2{}^2 + p_3{}^2)^{\frac{1}{2}} + \frac{\sigma}{2c_t}\frac{\omega_s f(\theta)}{\omega - \omega_s} - \frac{\omega}{c_t} = 0, \quad (7)$$

where θ is the angle between the vector $(p_1{:}p_2{:}p_3)$ and the local magnetic field.

In the following section attention will be directed toward rotationally symmetric systems, with rays travelling in meridian planes. It is appropriate, then, to use a cylindrical coordinate system, and (5) and (7), which are written in Cartesian coordinates, must be transformed. Since the φ component of $\nabla\psi$ is zero, (7) becomes

$$\Omega(\omega,p_r\,,\,p_z\,,\,r,z) = (p_r^{\,2} + p_z^{\,2})^{\frac{1}{2}} + \frac{\sigma}{2c_t}\frac{\omega_s f(\theta)}{\omega - \omega_s} - \frac{\omega}{c_t} = 0 \tag{8}$$

$$\theta = \eta - \xi$$

where $\eta = \tan^{-1} p_r/p_z$ and ξ is the polar angle of the local dc magnetic field (see Fig. 3). In a rotationally symmetric system the ray equations (5) transform into

$$dr/dw = \partial\Omega/\partial p_r, \qquad dz/dw = \partial\Omega/\partial p_z \tag{9a}$$

$$dp_r/dw = -\partial\Omega/\partial r, \qquad \partial p_z/dw = -\partial\Omega/\partial z \tag{9b}$$

IV. PARAXIAL RAY EQUATIONS AND REFRACTION IN CONVERGING AND DIVERGING MAGNETIC FIELDS

The discussion will now be restricted to the paraxial case; that is, only rays lying close to the symmetry axis and traveling almost parallel to it will be considered. Then

$$\eta \approx p_r/p_z\,.$$

Furthermore, the rotationally symmetric magnetic field will be assumed to be almost parallel to the axis ($\xi \ll 1$). Since $\theta \ll 1$,

$$f(\theta) \approx 1 - 2.5\,\theta^2;$$

and, when $\omega_M/\omega_H < 10$,

$$\omega_s \approx \omega_H + \omega_M(\theta^2/2).$$

If $\omega \approx \omega_s$ the denominator of the second term in (8) is small and

$$\frac{\partial}{\partial p_i}\frac{\sigma}{2c_t}\frac{\omega_s f(\theta)}{\omega - \omega_s} \approx \frac{\sigma}{2c_t}\frac{\omega_s f(\theta)}{(\omega - \omega_s)^2}\frac{\partial\omega_s}{\partial\theta}\frac{\partial\theta}{\partial p_i}$$

$$\frac{\partial}{\partial x_i}\frac{\sigma}{2c_t}\frac{\omega_s f(\theta)}{\omega - \omega_s} \approx \frac{\sigma}{2c_t}\frac{\omega_s f(\theta)}{(\omega - \omega_s)^2}\left(\frac{\partial\omega_s}{\partial H}\frac{\partial H}{\partial x_i} + \frac{\partial\omega_s}{\partial\theta}\frac{\partial\theta}{\partial x_i}\right),$$

where $p_i = p_r\,,\,p_z$ and $x_i = r,z$. Then

$$\frac{\partial\Omega}{\partial p_r} = \frac{p_r}{p_z} + \frac{\sigma\omega\omega_M}{2c_t p_z}\frac{\left(\dfrac{p_r}{p_z} - \xi\right)}{(\omega - \omega_H)^2} \tag{10a}$$

$$\frac{\partial\Omega}{\partial p_z} = 1, \tag{10b}$$

where only terms linear in p_r/p_z and ξ have been retained, in accordance

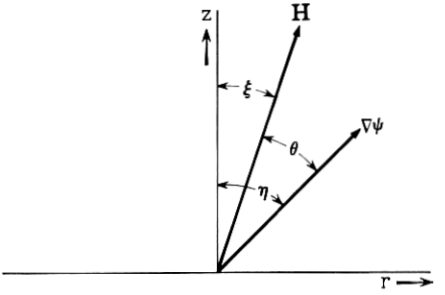

Fig. 3 — Orientation of the "local" wave vector $\nabla\psi$ relative to the local magnetic field.

with the paraxial approximation, and $\omega_s \approx \omega_H$ has been replaced by ω in the numerator of the second term in (10a). Similarly

$$\frac{\partial\Omega}{\partial r} = \frac{\sigma\omega}{2c_t}\frac{\gamma\dfrac{\partial H}{\partial r}}{(\omega - \omega_H)^2}. \tag{11}$$

From (9), (10) and (11) the paraxial ray equations are

$$\frac{dr}{dz} = \frac{1}{p_z}\left(p_r + \frac{\sigma\omega\omega_M}{2c_t}\frac{(p_r/p_z - \xi)}{(\omega - \omega_H)^2}\right) \tag{12}$$

and

$$\frac{dp_r}{dz} = -\frac{\sigma\omega}{2c_t}\frac{\gamma\dfrac{\partial H}{\partial r}}{(\omega - \omega_H)^2}. \tag{13}$$

In the paraxial approximation p_z is obtained directly from (8),

$$p_z \approx \frac{\omega}{c_t}\left(1 - \frac{\sigma}{2(\omega - \omega_H)}\right). \tag{14}$$

Consider now the case of a composite magnetic rod, the middle and outer sections having saturation magnetizations M and M' respectively, which is magnetized along its axis (see Fig. 4). The potential function for the dipolar field on the center line of the middle section, assuming

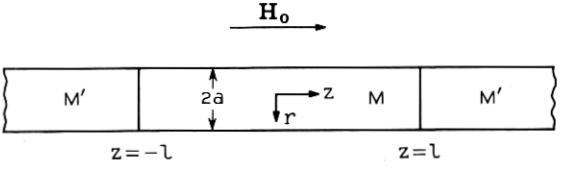

Fig. 4 — Composite rod configuration.

uniform magnetization, is[13]

$$V_D(z) = 2\pi(M - M')[\{(l - z)^2 + a^2\}^{\frac{1}{2}} - \{(l + z)^2 + a^2\}^{\frac{1}{2}} + 2z]$$

if the end effects of the outer sections are assumed to be negligible. Close to the axis the potential function is[14]

$$M_D(r,z) = V_D(z) - \frac{r^2}{4}\frac{\partial^2}{\partial z^2} V_D(z).$$

Assuming $(a/l)^2 \ll 1$, this leads to an internal field in the central region of the middle section

$$\begin{aligned} H &\approx H_0 - 6\pi(M - M')\frac{a^2}{l^2}\left(\frac{z^2}{l^2} - \frac{r^2}{2l^2}\right) \\ \xi &= \frac{H_r}{H_z} \approx \frac{6\pi(M - M')}{H_0}\frac{a^2}{l^2}\frac{zr}{l^2}, \end{aligned} \tag{15}$$

where only terms up to second order in z/l, r/l have been retained. Equation (15) shows that the internal field diverges with increasing $|z|$ when $M' < M$ and converges when $M' > M$. This result has been derived under the assumption of uniform magnetization. Actually the magnetization in the rod will itself be nonuniform, and nonuniformity of the field will be greater than is shown in (15).

A plane magnetoelastic wave is assumed to be propagating in the $+z$ direction at the midpoint of the rod, $z = 0$. Since p_r is then zero at this point and $\xi = 0$ from (15), it follows from (12) that $dr/dz = 0$. This means that the ray paths are parallel to the axis at $z = 0$. Elimination of p_r and p_z from (12), (13) and (14) leads to a second-order differential equation with variable coefficients for $r(z)$, and the ray path trajectories are obtained by solving this equation, subject to the assumed initial conditions. In this case a numerical integration is required for a complete description of the ray paths. If only the direction of refraction is required, the following simpler procedure may be used.

Substitution of (15) into (13) leads to

$$\frac{dp_r}{dz} = -\frac{3\sigma\omega}{4c_t}(\omega_M - \omega_{M'})\frac{a^2}{l^2}\frac{\dfrac{r}{l^2}}{\left(\omega - \omega_{H_m} + \dfrac{3}{2}(\omega_M - \omega_{M'})\dfrac{a^2}{l^2}\dfrac{z^2}{l^2}\right)^2}$$

where

$$\begin{aligned} \omega_M - \omega_{M'} &= \gamma 4\pi(M - M') \\ \omega_{H_m} &= \gamma\left(H_0 + \frac{3(M - M')}{4}\frac{a^2r^2}{l^4}\right). \end{aligned}$$

Over a small range of z close to $z = 0$ the value of r will not change appreciably along a ray path and dp_r/dz may be integrated directly, giving

$$p_r = -\frac{3\sigma\omega}{4c_t}\frac{(\omega_M - \omega_{M'})}{(\omega - \omega_{Hm})^2}\frac{a^2}{l^2}\frac{zr}{l^2} \tag{16}$$

to second order in z/l. This shows that the "local" wave vector deflects toward the axis with increasing z when $M' < M$ and away from the axis when $M' > M$. The corresponding slope of the ray path is found by substituting p_z and p_r from (14) and (16) into (12). That is

$$\frac{dr}{dz} = -A\left\{1 + \frac{\sigma\omega_M}{2(\omega - \omega_{H_m})^2\left(1 - \frac{\sigma}{2(\omega - \omega_{H_m})}\right)} + \frac{\omega_H}{\omega_{H_m}}\right\}\frac{a^2}{l^2}\frac{zr}{l^2} \tag{17}$$

up to terms of second order in z/l and r/l, where

$$A = \frac{3\sigma(\omega_M - \omega_{M'})}{4\left(1 - \frac{\sigma}{2(\omega - \omega_{H_m})}\right)(\omega - \omega_{H_m})^2}.$$

Equation (17) shows that when the field diverges ($M' < M$) magnetoelastic ray paths which are axial at $z = 0$ will converge, and vice versa. This is easily understood in terms of simple physical concepts. When the internal field decreases with increasing $|z|$ it increases with increasing r, as shown by (15). For a fixed frequency and propagation angle it is clear from Fig. 1 that the "refractive index" kc_t/ω decreases as H increases. If the anisotropy of the dispersion relation is ignored for the moment, this means that off-axis rays curve toward the region of higher "refractive index" closer to the axis. This isotropic effect is enhanced by anisotropy in the dispersion relation. When the wave vector is deflected from the magnetic field direction the ray path (defined by the group velocity) is deflected even further, as shown in Fig. 2, leading to an increased bending of the ray path.

This enhancement of the refractive effect by anisotropy is represented in (17) by the second and third terms under the bracket. In order to estimate the magnitude of these effects consider a YIG rod with $a/l = 0.1$ and $\omega_{H_0} = 2\pi \times 10^9$. For YIG $\sigma = 4 \times 10^6$ sec^{-1} and $\omega_M = 3.08 \times 10^{10}$. According to Schlömann[6] one-half the minimum frequency separation of the transverse magnetoelastic branches is

$$\omega_{\min} = (\sigma\omega_{cr}/2)^{\frac{1}{2}} \approx (\sigma\omega_{H_0}/2)^{\frac{1}{2}} = 1.12 \times 10^8.$$

If this value is assumed for $\omega - \omega_{H_m}$ the approximations used in obtaining (16) and (17) are valid when $z < 0.1l$, $r < 0.01l$. At $z = 0.1l$, $r =$

$0.01l$ the anisotropic terms in (17) are found to be an order of magnitude larger than the isotropic term, and the slope of the ray path is

$$\frac{dr}{dz} = -7.7 \times 10^{-4}.$$

On the basis of an extrapolation at this slope, the ray path should intersect the axis at $z \approx 10l$. The actual intersection would be closer than this because the ray path slope changes continuously with z. When the signal frequency is shifted closer to ω_{H_m}, an increased refraction results. For example, if

$$\omega - \omega_{H_m} = \omega_{\min}/3$$

the phase velocity of the magnetoelastic wave is, from (8), still within a few per cent of the acoustic velocity; but the slope of the ray path at $z = 0.1l$, $r = 0.01l$ is now

$$\frac{dr}{dz} = -3.2 \times 10^{-2}$$

and the extrapolated intersection point occurs at $z \approx 0.3l$. This large change in refractive power with decreasing $\omega - \omega_{H_m}$ is due to the resonance denominators in (17) and is an indication of the steep slopes of the wave vector surface, Fig. 2, in the vicinity of $\theta = 0$. The approximations used in obtaining (17) are, of course, not valid at resonance but are still at least marginally valid in the case considered here.

V. CONCLUSIONS

It has been shown that in a uniformly magnetized medium the phase and group velocities of a magnetoelastic wave are not collinear except

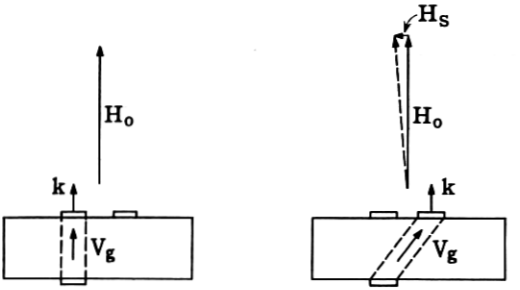

Fig. 5 — Beam steering by means of an auxiliary field.

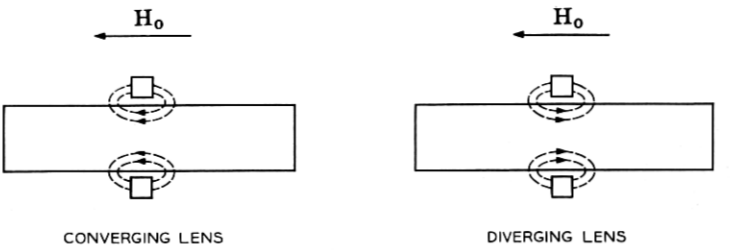

Fig. 6 — Examples of lens configurations.

when the wave vector is either parallel or normal to the magnetic field. This effect might be used for steering or switching an ultrasonic beam by means of an auxiliary field (see Fig. 5). Since the direction of the wave vector remains constant, the phase fronts remain parallel to the transducer faces.

Substantial refraction effects have been shown theoretically to occur in a nonuniformly magnetized medium. For the case of a magnetized rod it is found that paraxial magnetoelastic rays at frequency $\omega \approx \omega_H$

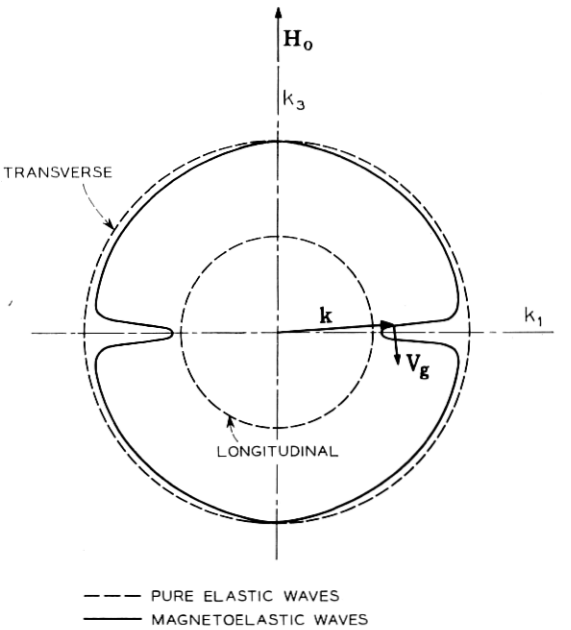

Fig. 7 — Wave vector surface for branch III of the dispersion diagram, at $\omega = \{\omega_H(\omega_H + \omega_M)\}^{\frac{1}{2}}$.

converge when the dipolar field and the applied field are opposing and diverge when the fields are aiding. In arriving at these results, the effects of losses and scattering due to imperfections have been ignored. By a similar analysis it can be shown that an annular permanent magnet or a circular coil encircling the rod will act as a converging lens if its field aids the applied field and as a diverging lens if the fields are opposing (Fig. 6). Paraplanar ray equations can be derived for radial propagation in an axially magnetized thin disk at a frequency $\omega \approx \{\omega_H(\omega_H + \omega_M)\}^{\frac{1}{2}}$. In this case the anisotropic refraction effect is found to oppose the isotropic effect and can even cause the net refraction to change sign. The physical reason for this can be seen by examining the wave vector surface for this case; see Fig. 7. This shows that a deflection of the wave vector away from $\theta = \pi/2$ produces a deflection of the group velocity in the opposite direction.

VI. ACKNOWLEDGMENTS

It is a pleasure to acknowledge many stimulating discussions with H. Seidel about propagation and ray optics in anisotropic media. This investigation was motivated by the work of W. Strauss, H. Matthews and R. T. Denton, with whom a number of helpful discussions have been held.

REFERENCES

1. Eshbach, J. R., J. Appl. Phys., *34*, 1963, p. 1298.
2. Strauss, W., J. Appl. Phys., *35*, 1964, p. 1022.
3. Damon, D., Bull. Amer. Phys. Soc. Ser. II, *9*, 1964, p. 260.
4. Schlömann, E., *Advances in Quantum Electronics*, Columbia University Press, New York, 1961, p. 437.
5. Joseph, R. I., and Schlömann, E., Bull. Amer. Phys. Soc. Ser. II, *9*, 1964, p. 260.
6. Schlömann, E., J. Appl. Phys., *31*, 1960, p. 1647.
7. Landau, L. D., and Lifshitz, E. M., *Electrodynamics of Continuous Media*, Pergamon Press, London, 1960, pp. 317–318.
8. Synge, J. L., *Geometrical Mechanics and de Broglie Waves*, Cambridge University Press, 1964, p. 56.
9. Landau, L. D., and Lifshitz, E. M., op. cit., p. 284.
10. Seidel, H., *Electromagnetic Theory and Antennas*, Pergamon Press, London, 1963, p. 565.
11. Burington, R. S., and Torrance, C. C., *Higher Mathematics*, McGraw-Hill, New York, 1939, p. 756.
12. Synge, J. L., Proc. Roy. Irish Acad., *63A*, 1963, p. 1.
13. Somerfeld, A., *Electrodynamics*, Academic Press, New York, 1952, p. 82.
14. Cosslett, V. E., *Introduction to Electron Optics*, Oxford University Press, London, 1950, p. 35.